Scientific Research Publishing

Engineering, 2026, 18(11), 490-505
https://www.scirp.org/journal/eng
ISSN Online: 1947-394X
ISSN Print: 1947-3931

Performance Evaluation of OFDM Transmission and Techno-Economic Feasibility of 5G NR Deployment: Case of Telecel Faso

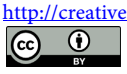
Wendpuiré Ousmane Compaoré[1,2*], Izak Kévin Compaoré[1,3], Maxime Kafando[3], Zacharie Koalaga[2]

[1]Materials Helio-Physics and Environment Laboratory (LaMHE), Nazi Boni University, Bobo-Dioulasso, Burkina Faso
[2]Materials and Environment Laboratory (LaME), Joseph Ki-Zerbo University, Ouagadougou, Burkina Faso
[3]Technical Division, Telecel Faso, Bobo-Dioulasso, Burkina Faso
Email: *cwousmane@yahoo.fr

How to cite this paper: Compaoré, W.O., Compaoré, I.K., Kafando, M. and Koalaga, Z. (2026) Performance Evaluation of OFDM Transmission and Techno-Economic Feasibility of 5G NR Deployment: Case of Telecel Faso. *Engineering*, **18**, 490-505.
https://doi.org/10.4236/eng.2026.1811027

Received: September 15, 2026
Accepted: November 10, 2026
Published: November 13, 2026

Copyright © 2026 by author(s) and Scientific Research Publishing Inc.
This work is licensed under the Creative Commons Attribution International License (CC BY 4.0).
http://creativecommons.org/licenses/by/4.0/



Open Access

Abstract

This paper evaluates the technical and economic feasibility of deploying 5G NR on the network of the Burkinabè mobile operator Telecel Faso through a MATLAB-based simulation of an OFDM transmission chain. The study quantifies three major technological bottlenecks: Peak-to-Average Power Ratio (PAPR) reduction, Doppler effect tolerance under high mobility, and spatial diversity gains provided by Multiple-Input Multiple-Output (MIMO) techniques. The simulation results demonstrate that clipping at an 8 dB threshold reduces the PAPR by 2.5 dB, significantly improving the power efficiency of base station power amplifiers—a critical operational requirement given local energy constraints. Regarding mobility, adopting numerology $\mu = 2$ with a 60 kHz subcarrier spacing preserves link integrity at speeds up to 350 km/h, ensuring seamless service continuity along major road corridors. Furthermore, the 2×2 Alamouti space-time block-coding scheme yields a 15 to 18 dB diversity gain over a Rayleigh fading channel, successfully eliminating error floors in dense urban environments. Overall, this techno-economic characterization confirms that a phase-one 5G NR rollout is immediately feasible via a software upgrade of the legacy Huawei RAN infrastructure for an estimated investment of 10 million XOF.

Keywords

OFDM, 5G NR, PAPR, Doppler Effect, MIMO, Telecel Faso, Energy Efficiency

1. Introduction

The evolution of mobile networks from 4G LTE to 5G NR is driven by an exponential growth in data traffic, propelled by the ubiquity of high-definition video streaming, the proliferation of Internet of Things (IoT) devices, and the emergence of ultra-low latency applications [1] [2]. To overcome the spectral efficiency constraints inherent to traditional multiplexing schemes (FDM, TDM, CDMA), Orthogonal Frequency Division Multiplexing (OFDM) has established itself as the core physical layer standard [3]-[5]. Utilizing subcarriers that overlap at right angles, OFDM enhances spectral efficiency and offers strong protection against multipath fading that varies with frequency.

Nonetheless, moving to 5G NR poses considerable operational and financial difficulties, especially in Sub-Saharan Africa, where mobile networks are mainly designed for 4G. For a company such as Telecel Faso, which is the third-largest provider in Burkina Faso with close to 3 million subscribers, transitioning to 5G NR involves a practical approach focused on optimizing capital expenditure and ensuring compatibility with existing systems. The deployment of late-generation Huawei radio equipment (such as the BBU BTS5900 and advanced RRUs) enables a Non-Standalone (NSA) migration path via a straightforward software upgrade [6] [7]. Consequently, the core research challenge shifts from determining whether 5G NR is achievable to precisely characterizing the physical-layer requirements and economic viability of its integration.

While the scientific literature extensively addresses physical-layer bottlenecks in OFDM systems—such as Peak-to-Average Power Ratio (PAPR) reduction through clipping, SLM, or PTS techniques [8] [9], Doppler shift mitigation using flexible 5G NR numerologies, and spatial diversity gains via MIMO technologies [3] [5]—few studies holistically combine these physical parameters within a simulation framework tailored to the operational realities of a West African mobile operator.

This paper presents a techno-economic feasibility study for the deployment of 5G NR at Telecel Faso, supported by a MATLAB-based simulation of an end-to-end OFDM transmission chain. The study sequentially quantifies the energy efficiency gains achieved through PAPR reduction, link robustness under high highway mobility scenarios, and diversity gains in dense urban channels. These physical performance metrics are then translated into a practical deployment roadmap.

The remainder of this paper is organized as follows: Section II outlines the system model and MATLAB simulation methodology; Sections III through V we adress analyze the empirical results regarding PAPR, Doppler tolerance, and MIMO diversity; In Section VI, we present the techno-economic feasibility assessment for Telecel Faso, followed by concluding remarks in Section VII.

2. Problem Statement

The advent of fifth-generation mobile networks (5G NR) marks a major technological breakthrough, promising ultra-high data rates, reduced latency, and un-

precedented spectral flexibility. However, in sub-Saharan Africa, simply copying and pasting Western or Asian models cannot achieve the deployment of these technologies. For service providers such as Telecel Faso in Burkina Faso (with around 3 million customers), the transition to 5G NR must reconcile radio performance requirements with the economic constraints of existing infrastructure (Huawei BBU BTS5900 and RRU equipment). In practice, this transition faces three major technological hurdles:

- Energy inefficiency (high PAPR).
- Vulnerability to mobility (Doppler effect).
- Urban error floor (multiple paths).

To address these shortcomings, this article uses Modeling and MATLAB simulation to evaluate an OFDM transmission chain adapted to the context of Telecel Faso.

3. OFDM Principles and 4G/5G NR Physical Context

Characterizing the mobile radio channel represents an indispensable prerequisite for cellular network dimensioning. Unlike stable, guided wired links [8], the wireless environment imposes severe propagation constraints: path loss degrades the signal-to-noise ratio (SNR) as a function of distance; multipath propagation in urban environments causes frequency-selective fading and inter-symbol interference (ISI), while user mobility induces Doppler spread that disrupts frequency synchronization. To address this threefold physical challenge, Cyclic Prefix Orthogonal Frequency Division Multiplexing (CP-OFDM) was standardized by 3GPP as the baseline waveform for 4G LTE and 5G NR down link transmissions [2] [10].

Conceptually, an OFDM system divides the channel bandwidth into a large number of orthogonal subcarriers, efficiently synthesized via Inverse Fast Fourier Transform (IFFT) at the transmitter and extracted via FFT at the receiver [4]. Strict orthogonality between two subcarriers with frequencies f_k and f_l is guaranteed over a symbol duration T_S provided their subcarrier spacing Δf satisfies $\Delta f = 1/T_S$. This managed overlap removes the passive guard bands needed by traditional FDM, thus enhancing spectral efficiency.

To reduce the delay spread of the channel, a cyclic prefix (CP) is added to the beginning of every symbol. By absorbing inter-symbol interference, the CP converts the linear convolution of the channel into a circular convolution, reducing receiver equalization to a straightforward complex division per subcarrier.

Table 1 below summarizes the main differences between 4G LTE and 5G NR.

Table 1. Summary Comparison of 4G LTE/5G NR Parameters.

Parameters	4G LTE	5G NR
Δf Spacing	15 kHz (fixed)	15 - 120 kHz
Max Bandwidth	20 MHz	400 MHz
MIMO	8 × 8 max	64 - 256 ante
Latency	10 ms max	<1 ms

Furthermore, OFDM inherently aligns with multi-antenna (MIMO) architectures. Due to the fact that every subcarrier undergoes uniform fading, the spatial processing needed to merge the streams from multiple antennas is greatly simplified, making it possible to implement large-scale MIMO systems that are vital for increasing capacity in crowded urban environments.

However, there are two significant physical constraints that practical OFDM setups encounter. The first issue is that the coherent addition of subcarriers results in a high Peak-to-Average Power Ratio (PAPR), pushing power amplifiers into nonlinear areas of operation, which presents a major financial and energy efficiency challenge for base station implementations. The second issue is that high sensitivity to frequency shifts caused by Doppler effects disrupts the orthogonality between subcarriers, leading to inter-carrier interference (ICI) in situations with high mobility.

As a result, moving from a fixed 4G LTE framework to a more adaptable 5G NR structure necessitates addressing these physical obstacles while maintaining compatibility with existing systems. Optimizing these physical layer parameters in Table 1 forms the core of the techno-economic feasibility study conducted on Telecel Faso's network.

4. Simulation Methodology and System Architecture

To translate the physical principles of CP-OFDM discussed in Section II into quantifiable performance indicators, an end-to-end transmission chain was implemented within the MATLAB environment [11]. The decision to build a custom algorithmic framework—bypassing proprietary, commercial 5G toolboxes—serves a dual scientific and operational objective: it ensures granular control over every processing block (QAM mapping, IFFT synthesis, CP insertion, channel modeling, FFT, equalization, and demodulation) while faithfully replicating the core processing sequences executed by the Digital Signal Processors (DSP) within the Huawei BBU BTS5900 baseband units [12] currently deployed across Telecel Faso's network.

To balance computational efficiency with physical accuracy, the baseline physical model employs a 64-point FFT core configured with 52 active subcarriers (a scaled, representative model of the full-scale 2048-point LTE standard), appended with a 16-sample cyclic prefix ($CP \approx 25\%$). The physical layer chain supports QPSK, 16-QAM, and 64-QAM modulation schemes.

Performance evaluation is conducted across two complementary propagation environments:

- An Additive White Gaussian Noise (AWGN) channel: serving as the theoretical baseline for PAPR characterization and constellation decision threshold validation.
- A 3-tap frequency-selective Rayleigh fading channel: defined by relative delay profiles of $[0,1,3]$ samples and power gain profiles of $[1,1.5,0.25]$, accurately capturing the multipath reflection profile characteristic of Bobo-Dioulasso's dense urban topology.

To evaluate Doppler shift resilience and lay the groundwork for 5G NR migration dimensioning, the four 3GPP-standardized numerologies $\mu \in \{0,1,2,3\}$,

corresponding to subcarrier spacings Δf from 15 to 120 kHz, were integrated into the simulator. Each operational scenario undergoes Monte Carlo evaluation over 1,000 consecutive OFDM symbols per Signal-to-Noise Ratio (SNR) step, swept across a range of 0 to 30 dB. Table 2 summarizes the complete parameter set governing the simulation platform. They are aligned with the reference 5G NR numerology ($\mu = 0.15$ kHz subcarrier spacing, 20 MHz channel bandwidth).

Table 2. Main parameters of simulated OFDM chain.

Parameters	Retained Values
Carrier frequency	3.5 GHz (band n78)
Sampling rate	30.72 MHz
FFT size	2048 for μ = 0; 2048/ 2^{μ} for other numerologies
Useful subcarriers	1272 (106 PRBs) for $\mu = 0$
Cyclic Prefix (normal CP)	144 samples for $\mu = 0$
CP duration $\mu = 0$ (15 kHz)	4.69 μs
CP duration $\mu = 1$ (30 kHz)	2.34 μs
CP duration $\mu = 2$ (60 kHz)	1.17 μs
CP duration $\mu = 3$ (120 kHz)	0.59 μs
Modulations	QPSK, 16 – QAM, 64 – QAM
5G NR numerologies	$\mu = 0, 1, 2, 3$(15 to 120 kHz)
Channel	Rayleigh, 3 taps
Doppler model	Jakes
Swept velocities	3 to 500 km/h (maximum Doppler frequency of approximately 1.62 kHz)
Swept SNR	0 to 30 dB
OFDM symbols per SNR point	1000
Rayleigh realisations per SNR point	50

Figure 1 shows the general architecture of simulated OFDM chain.

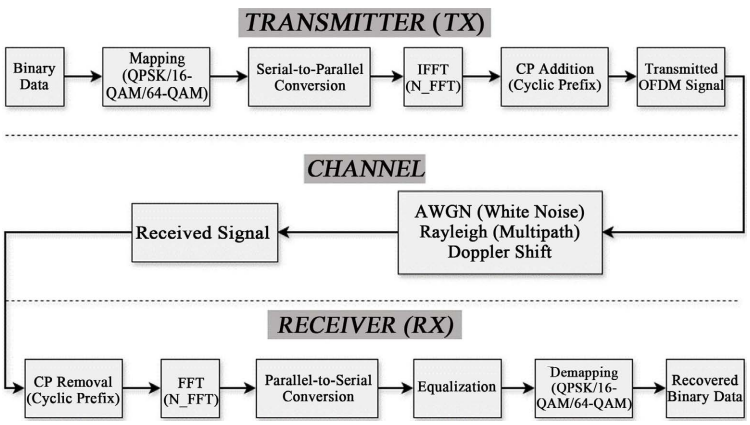


Figure 1. Simulated OFDM transmission chain architecture.

The sampling rate of 30.72 MHz corresponds to a 20 MHz bandwidth, that is, a ratio fs/B of 1.536. The 3.5 GHz carrier lies in band n78, which constitutes one of the principal axes of worldwide 5G NR deployment and is envisaged for the deployment of Telecel Faso. The Doppler model retained is Jakes' model, conventionally employed for mobile channels. At 500 km/h and 3.5 GHz, the maximum Doppler frequency reaches approximately 1.62 kHz, that is, nearly 11% of the subcarrier spacing for $\mu = 0$. This ratio regulates the interference between carriers and the resilience of the system at elevated speeds. The power-delay profile is adjusted so that the total of the powers equals one, ensuring a consistent reference SNR no matter the setup.

In exploring each physical limitation discussed in the following sections (PAPR, Doppler shift, and MIMO application), the approach follows a thorough four-step process: first, empirical observation of the physical effect through simulation; second, application of a specific mitigation strategy; third, quantitative assessment of the resulting compromises; and lastly, development of practical engineering suggestions. This organized method provides a consistent foundation for evaluating physical limitations before they are integrated into the techno-economic viability analysis in Section VII.

5. Results: SISO Chain Validation and PAPR Evaluation

5.1. Functional Verification of the SISO Chain

The dependability of the SISO OFDM simulator was confirmed by thoroughly testing four essential physical metrics. First, the consistency of QPSK mapping was confirmed by the exact alignment of the symbols onto theoretical constellation coordinates $\left(\pm\sqrt{2}, \pm\sqrt{2}\right)$ illustrated in Figure 2. Second, the spectral analysis validates the energy confinement within the useful bandwidth and the expected attenuation across the lateral guard subcarriers.

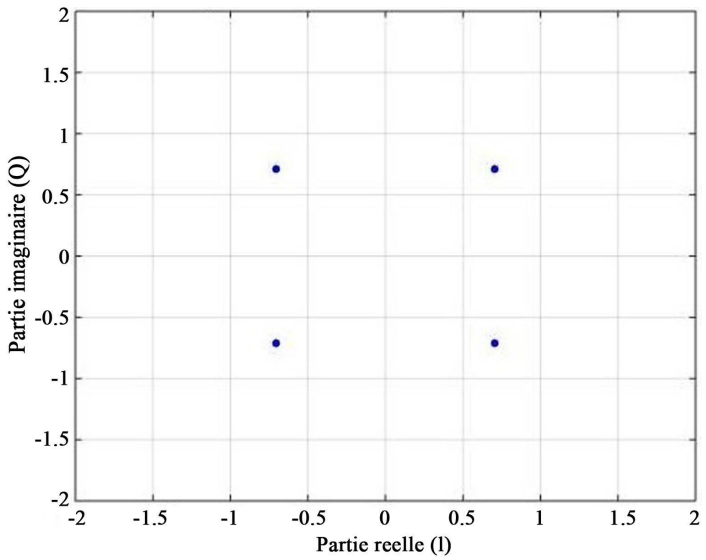


Figure 2. QPSK constellation diagram.

Third, the description of the Bit Error Rate (BER) in an Additive White Gaussian Noise (AWGN) channel shows a complete match with theoretical predictions, reaching the desired BER of 10^{-6} at a Signal-to-Noise Ratio (SNR) of near 12 dB for QPSK. Furthermore, scaling up the modulation order (from QPSK to 16-QAM and 64-QAM) introduces a logical SNR penalty of ~16 dB to maintain this baseline performance level (BER = 10^{-6}), accurately illustrating the classic trade-off between spectral efficiency and noise robustness.

Finally, evaluation over the 3-tap frequency-selective Rayleigh fading channel, shown in Figure 3, highlights the intrinsic vulnerability of the SISO link. The lack of spatial diversity severely degrades the slope of the BER curve, sustaining a relatively high error rate (~10^{-4} to 10^{-5}) even at high SNR regimes (30 dB). This behavior empirically confirms the necessity of introducing spatial diversity mechanisms (MIMO) to guarantee a reliable quality of service in dense urban environments.

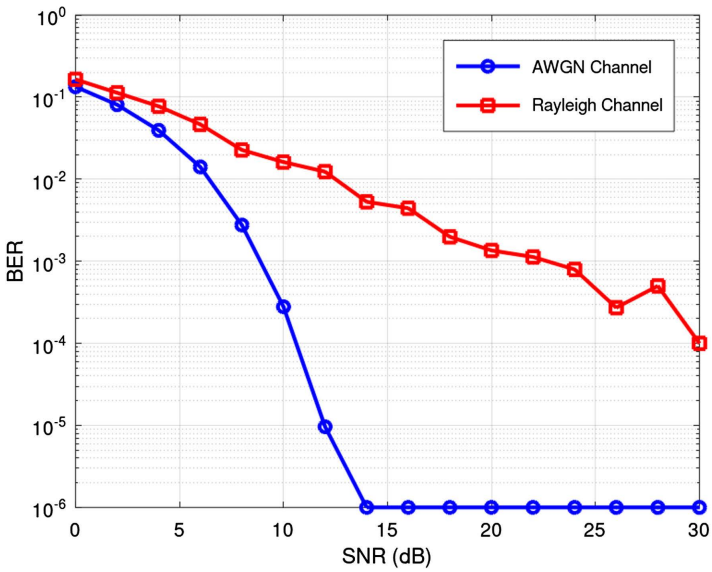


Figure 3. BER performance of an OFDM SISO system in AWGN and Rayleigh channels.

5.2. PAPR Characterization and Mitigation

Evaluating the peak-to-average power ratio (PAPR) through the complementary cumulative distribution function (CCDF) gives an average PAPR of 6.7 dB, with peaks reaching10.5 dB. More critically, about 20% of the generated OFDM symbols exceed a 9 dB threshold. This constraint forces a severe output back-off (OBO) on the power amplifiers (PAs) integrated into the Remote Radio Units (RRUs). The PAs must then operate well below saturation, in a low-efficiency regime, to avoid non-linear distortion and adjacent-channel spectral regrowth.

To relieve this bottleneck without hardware overhead or receiver-side signaling (side information), we evaluated amplitude clipping [9] over several clipping ratios (CR).

Clipping is applied to the time-domain signal after oversampling by a factor of

4, that is, at a sampling frequency of 122.88 MHz, which limits spectral regrowth. The clipping threshold CR_{dB} is defined as the ratio, in decibels, between the peak power and the targeted mean power. For the 8 dB threshold used throughout this study, the amplitude limit given by (1):

$$A_{clip} = \sqrt{P_{avg} \cdot 10^{\frac{CR_{dB}}{10}}} \quad (1)$$

where P_{avg} denotes the mean power of the OFDM signal. Any sample whose amplitude exceeds A_{clip} is set to this value, its phase being preserved. By construction, the PAPR of the clipped signal is approximately bounded by CR_{dB}; the small deviation comes from the reduction of the mean power after clipping.

Setting the clipping threshold at 8 dB yields the best operational trade-off. It reduces the peak PAPR by 4 dB at the cost of a marginal BER degradation, equivalent to an SNR penalty of 1 to 1.5 dB at the target BER of 10^{-3}. On the other hand, applying stronger clipping at 6 dB results in significant in-band distortion and a bit error rate penalty ranging from 2 to 3 dB. The effect of the 8 dB threshold on the PAPR distribution is shown in Figure 4.

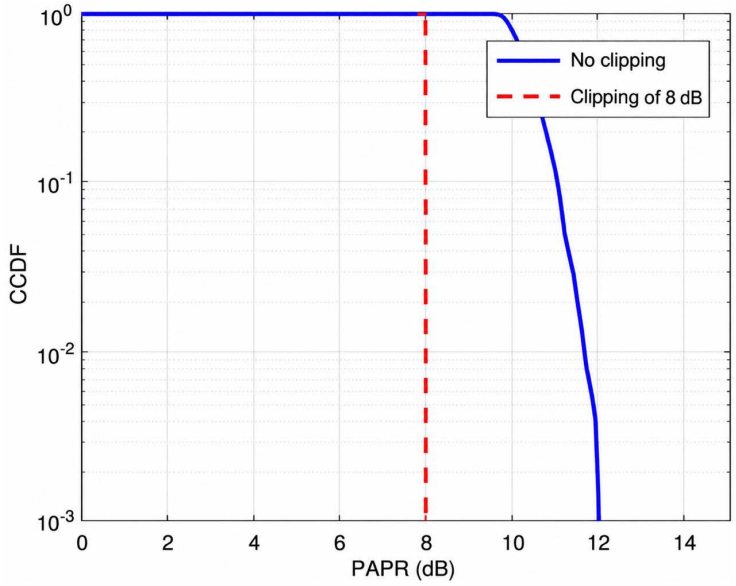


Figure 4. CCDF of PAPR before and after clipping at 8 dB.

The transmitter quality parameters obtained at 8 dB are summarized in Table 3.

Table 3. Transmitter quality after clipping at 8 dB.

Parameter	Measured value	Reference limit (3GPP)
EVM (Error Vector Magnitude)	5%	8% (64-QAM)
ACLR/ACPR (Adjacent Channel Leakage Ratio)	−35 dBc	−30 dBc

These results indicate that clipping at 8 dB remains compatible with the transmitter quality requirements defined by 3GPP, subject to verification of the normative limits cited above.

From an operational standpoint, this mitigation can be deployed through a software or firmware update of the DSP cards of the Huawei BBUs, without any hardware change. By suppressing power peaks by 2.5 dB, the operator can relax the PA linearity constraints. Across the Telecel Faso RAN footprint, the improved RRU power efficiency translates directly into lower site energy consumption and a measurable reduction in operational expenditure (OPEX).

6. Results: Doppler Effect, Numerology, and Channel Coding

6.1. Mobility Sensitivity and Impact of 5G NR Numerology

In a mobile environment, a terminal moving at velocity v experiences a Doppler frequency shift in Equation (2)

$$f_d = (v * f_c)/c \tag{2}$$

relative to the carrier frequency f_d (c being the speed of light). This frequency shift destroys the orthogonality among subcarriers and introduces Inter-Carrier Interference (ICI), directly degrading the Signal-to-Interference-plus-Noise Ratio (SINR).

Evaluating the physical flexibility of 5G NR demonstrates that the baseline numerology $\mu = 0$ (Δf = 15 kHz, inherited from 4G LTE) suffers severe BER degradation at speeds exceeding 200 km/h. Conversely, adopting numerology $\mu = 2$ (Δf = 60 kHz) widens the subcarrier spacing, accommodating significantly higher Doppler spread and maintaining a stable BER up to extreme speeds of 350 km/h shows in Figure 5.

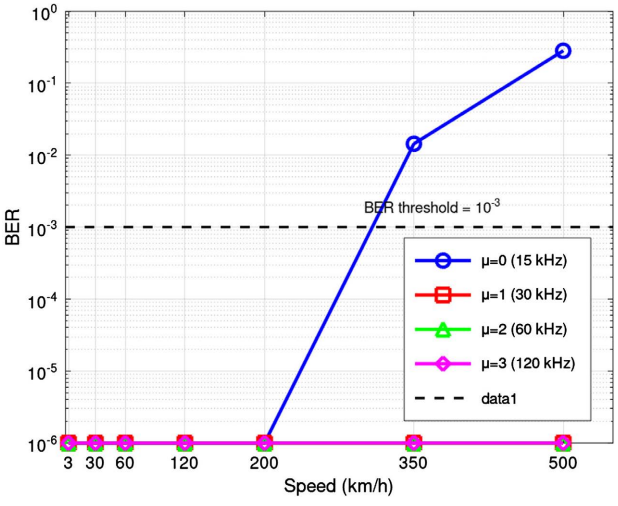


Figure 5. BER vs. Speed for the four 5G NR numerologies.

Under static conditions (AWGN channel), all four numerologies exhibit virtually identical performance. Consequently, selecting a wider subcarrier spacing

serves as an optimization dedicated strictly to mobility tolerance, incurring no performance penalty under stationary conditions. For Telecel Faso, deploying numerology $\mu = 2$ provides a generous reliability margin across Burkina Faso's major intercity highway corridors (where vehicular speeds typically range from 80 to 130 km/h).

6.2. Impact of Channel Coding (FEC) in Selective Fading Environments

To fortify the radio link against deep frequency-selective Rayleigh fading and residual ICI, a rate $R = 1/2$ convolutional Forward Error Correction (FEC) scheme paired with Viterbi soft-decision decoding [13] was integrated into the transmission chain.

Over an AWGN channel, this coding scheme yields a net $6\,dB$ coding gain at equivalent BER targets. Over the frequency-selective Rayleigh channel, the impact of FEC is crucial: it eliminates the asymptotic error floor observed in uncoded transmissions (BER $\approx 10^{-3}$ to 10^{-4}), achieving high service reliability (BER = 10^{-6}) at a moderate SNR range of 16 to 18 dB.

7. Results: Spatial Diversity (MIMO) and Beamforming

7.1. Spatial Diversity Gain of the 2 × 2 Alamouti Scheme

To mitigate frequency-selective Rayleigh fading without adding uplink feedback overhead for channel state information at the transmitter (CSIT), we evaluated the Alamouti space-time block code (STBC) in a 2 × 2 MIMO configuration [7]. The simulations show a clear improvement over the baseline SISO link. At the target Bit Error Rate (BER = 10^{-3}), the 2 × 2 MIMO system provides a net spatial diversity gain of 15 to 18 dB over the Rayleigh channel. It also reaches the reliability threshold at a signal-to-noise ratio (SNR) of only 10 to 12 dB, which is almost the same as what an ideal additive white Gaussian noise (AWGN) channel achieves in Figure 6.

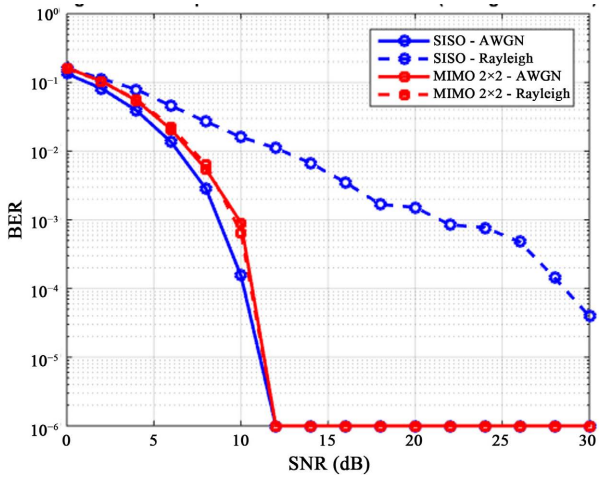


Figure 6. BER comparison: SISO vs. 2 × 2 MIMO in AWGN and Rayleigh channels.

Physically, the improvement comes from diversity combining, which reduces the probability of deep fades and of outage, thereby eliminating the structural error floor characteristic of SISO transmissions. Combining does not, however, create a line-of-sight component: each individual link still follows a Rayleigh distribution, and the gain lies in the lower probability that all branches are in a deep fade at the same time.

7.2. Beamforming and Array Gain

Unlike Alamouti MIMO, which exploits spatial diversity to fight fading, beamforming applies progressive phase and amplitude weightings across an antenna array to synthesize a directional radiation pattern [7]. By generating constructive interference in the intended direction and destructive interference elsewhere, beamforming delivers a theoretical array gain expressed as $10 \times \log_{10} \mathrm{N}$ dB, where N represents the number of radiating elements.

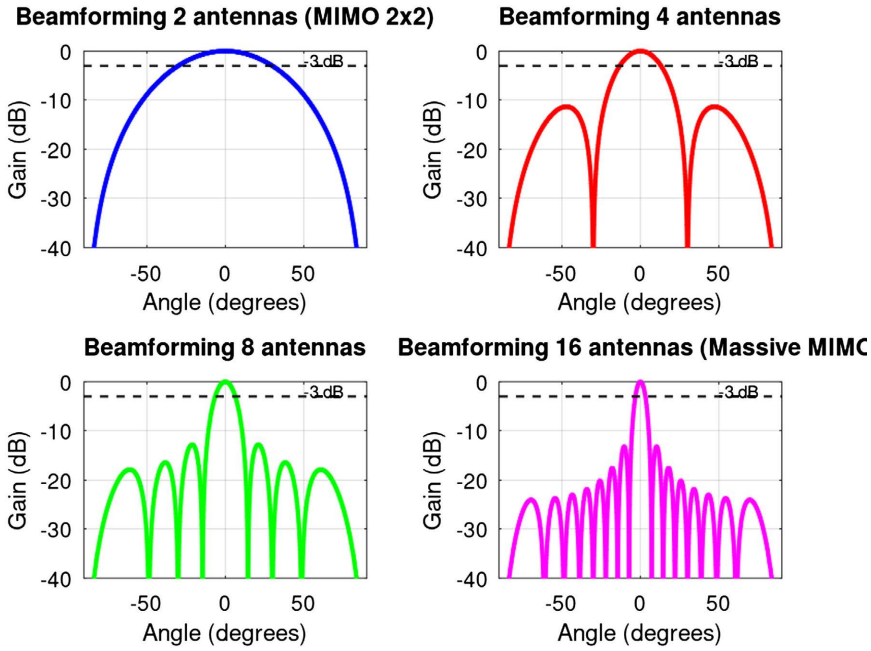


Figure 7. Radiation patterns for 2, 4, 8, and 16 element antenna arrays.

Simulating array topologies with $N \in \{2,4,8,16\}$ elements confirms boresight power gains of 3, 6, 9, and 12 dB, respectively, in **Figure 7**. The $N = 8$ configuration (9 dB power gain) represents an optimal trade-off for retrofitting dense urban sites across Telecel Faso's footprint, while the $N = 16$ setup lays the groundwork for Massive MIMO deployment [14]. Applying beamforming to three representative deployment scenarios illustrated in **Figure 8** highlights the flexibility of directional coverage targeting:

- Dense Urban Core in blue (e.g., Bobo-Dioulasso): Broad, high-resilience beams for rich multipath environments.
- Suburban/Peripheral Zones in red: Energy-concentrated beams to extend cov-

erage to cell-edge users.

- National Highway RN1 Corridor in green: Narrow, elongated beams aligned with the transit route to maintain link budget for high-speed mobility.

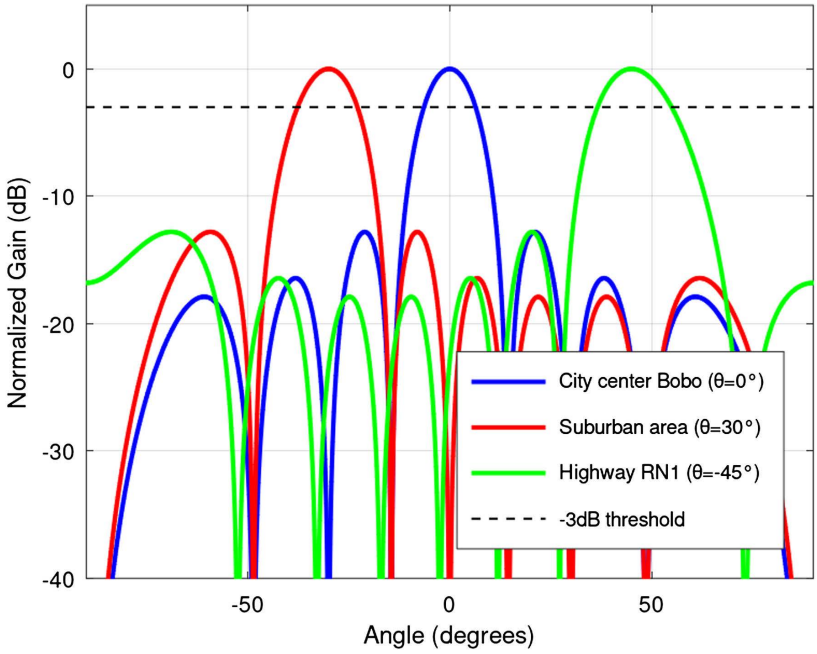


Figure 8. Example of scoring across three zones: the center of Bobo in blue, a peripheral district in red, and the RN1 highway in green.

7.3. Synergy and Additivity of Physical Layer Protections

Table 4 summarizes the SNR values required to reach a BER of 10^{-3} and of 10^{-6}

Table 4. Required SNR by configuration.

Configuration	SNR at BER = 10^{-3}	SNR at BER = 10^{-6}
SISO without FEC	>30 dB (floor)	Not reached
FEC only	16 to 18 dB	16 to 18 dB
MIMO 2 × 2 only	10 to 12 dB	10 to 12 dB
MIMO + FEC	8 to 10 dB	8 to 10 dB

Compared with SISO without FEC, whose BER of 10^{-3} is not reached below 30 dB, the combination of MIMO and FEC yields a gain of at least 20 dB. Adding FEC to a 2 × 2 MIMO link lowers the threshold by approximately 2 dB on the central values, which reflects a complementary effect between spatial diversity and error correction. This difference, however, is of the order of the measurement variability and should be confirmed by complementary simulations.

A comparative synthesis of the physical layer techniques reveals a clear performance hierarchy and a remarkable synergy among mechanisms:

- Forward Error Correction (FEC) eliminates the Rayleigh error floor but re-

quires an SNR of 16 to 18 dB to hit BER = 10^{-6}

- 2 × 2 Alamouti MIMO outperforms FEC alone, reaching the same target at 10 to 12 dB.
- Combining both techniques (2 × 2 MIMO + FEC) produces an additive effect, achieving a cumulative gain of 20 to 22 dB over uncoded SISO.

The additional 2 dB synergy gain arises from the soft-decision Viterbi decoder processing a signal whose deep fading dips have already been smoothed out by spatial diversity. These empirical findings demonstrate that deploying MIMO and beamforming is not merely an optional software optimization, but an essential engineering pillar to guarantee coverage and capacity in a commercial 5G NR deployment.

8. Discussions: 5G NR Deployment Feasibility

The preceding results allow for the definition of an adaptive zoning model, summarized in Table 4, which pairs each geographic zone type with a specific numerology, antenna configuration, and 5G NR service mix aligned with the measured empirical constraints.

8.1. Validation of Results against Literature

To establish a clear theoretical baseline for the proposed simulator, this section reviews core physical-layer techniques tailored to Sub-6 GHz radio propagation. Rather than addressing non-terrestrial or optical propagation environments, the following synthesis isolates the fundamental building blocks of modern terrestrial transceivers: frame-level OFDM signaling, space-time diversity via the Alamouti scheme, and adaptive channel estimation/equalization over Rayleigh fading channels.

8.2. Deployment Feasibility for Telecel Faso

Based on the obtained results, a progressive three-phase deployment scenario is proposed. The first phase (0 - 3 months) consists of an NSA software upgrade on Huawei BTS5900 BBUs without hardware replacement, requiring an estimated investment of 10 million XOF across six pilot sites in Ouagadougou and Bobo-Dioulasso. The second phase (3 - 6 months) entails deploying beamforming-capable Active Antenna Units (AAUs) for an estimated investment of at least 24 million XOF. Finally, the third phase (6 - 12 months) extends coverage along major highway corridors and rural zones while preparing for migration toward a 5G Standalone architecture. Table 5 presents the cost estimate for each deployment phase. The total corresponds to the sum of the three phases.

An inspection of the equipment conducted during field training confirms the hardware compatibility of Huawei BBUs and RRUs [12] with Sub-6 GHz NSA mode, subject to a firmware update and regulatory spectrum allocation by ARCEP Burkina Faso [15]—specifically band n78 (3.5 GHz) and band n1 (2.1 GHz), reallocable via Dynamic Spectrum Sharing [5].

Table 5. Cost estimate by phase.

Phase	Scope and equipment (Huawei)	Number of sites	Estimated cost (FCFA)	Justification
Phase 1: short term (0 to 3 months)	NSA software activation of existing BBU BTS5900, RTN backhaul	6 sites (Ouagadougou and Bobo-Dioulasso)	10,000,000	Firmware update of existing BBUs. No hardware replacement. Existing backhaul reinforced.
Phase 2: medium term (3 to 6 months)	Active antennas AAU 5613 (Massive MIMO and beamforming) and RRU radio swap for the sub-6 GHz 5G band	30 dense urban sites	450,000,000	Estimated unit cost of 15 M FCFA per site (AAU, RRU and installation). Equipment required for beamforming and 5G data rates.
Phase 3: long term (6 to 12 months)	Extension of road axes (RN1 and others), deployment of the 5GC core (Huawei)	Approximately 100 sites, plus the core network	2,500,000,000	Average cost of 20 M FCFA per site for rural areas, plus 500 M FCFA for the 5GC core.
TOTAL ESTIMATE	Overall 5G NR extension project for Telecel Faso	Approximately 136 sites (national scale)	2,960,000,000 (≈2.96 billion)	Sum of the three phases.

8.3. Study Limitations and Future Perspectives

This study includes several recognized limitations: the 3-tap Rayleigh channel serves as a simplified approximation of the physical radio environment, channel estimation is assumed to be ideal (whereas real-world estimation via DMRS pilots would introduce an additional 1 to 2 dB SNR degradation), and inter-cell interference is not explicitly modeled. These limitations define clear avenues for future research, including neural network-based channel estimation [16], in-situ propagation measurements in Bobo-Dioulasso, and multi-cell modeling incorporating ICIC/eICIC mechanisms [17].

9. Conclusions

This paper presented an in-depth simulation-based characterization of an OFDM transmission chain operating under LTE/5G NR requirements to resolve three fundamental physical layer bottlenecks: Peak-to-Average Power Ratio (average PAPR of 6.7 dB, reduced by 2.5 dB via an optimal 8 dB clipping threshold), Doppler tolerance (link integrity guaranteed up to 350 km/h using numerology $\mu = 2$), and spatial diversity exploitation (15 to 18 dB gain delivered by the 2×2 Alamouti MIMO scheme over a Rayleigh fading channel). The underlying techno-economic evaluation demonstrates that a Phase-1 5G\NR deployment is immediately actionable for Telecel Faso via a software-only upgrade of existing radio infrastructure, requiring an initial investment estimated at 10 million XOF.

Beyond its direct operational impact on the Burkinabè market, this research establishes that a contextualized, adaptive deployment model—in contrast to uniform rollouts modeled after mature markets—represents the most viable trajectory for mobile operators in developing nations. Future research avenues emerging from this study, including artificial intelligence-driven channel estimation

[16], extension into millimeter-wave spectrum bands [17], and network slicing modeling for URLLC applications in telemedicine and connected agriculture, set the groundwork for next phases of this infrastructure evolution.

Acknowledgements

The authors express their gratitude to the Technical Directorate of Telecel Faso in Bobo-Dioulasso for providing access to radio site infrastructure and operational network data, which proved essential for contextualizing and validating this techno-economic study.

Author Contributions

Conceptualization, methodology, and formal analysis: Wendpuiré Ousmane Compaoré. Research and data management: Izak Kévin Compaoré and Maxime Kafando. Analytical review: Izak Kévin Compaoré and Maxime Kafando. Supervision: Zacharie Koalaga. Writing, revision, and editing: Wendpuiré Ousmane Compaoré, Izak Kévin Compaoré, and Zacharie Koalaga. All authors have read and approved the final version of manuscript.

Conflicts of Interest

The authors declare no conflicts of interest regarding the publication of this paper.

References

[1] Jiang, W., Zhou, Q., He, J., Habibi, M.A., Melnyk, S., El-Absi, M., *et al*. (2024) Terahertz Communications and Sensing for 6G and Beyond: A Comprehensive Review. *IEEE Communications Surveys & Tutorials*, **26**, 2326-2381. https://doi.org/10.1109/comst.2024.3385908

[2] Anughna, N. and Ramesha, M. (2022) Performance Analysis on 5G Waveform Candidates for MIMO Technologies. 2022 *IEEE* 2*nd Mysore Sub Section International Conference* (*MysuruCon*), Mysuru, 16-17 October 2022, 1-8. https://doi.org/10.1109/mysurucon55714.2022.9971805

[3] Proakis, J.G. and Salehi, M. (2008) Digital Communications. 5th Edition, McGraw-Hill.

[4] Boudoumi, S. and Chaib, M. (2016) Modélisation d'un système de transmission COFDM sous l'environnement Simulink Matlab. Mémoire de fin d'études d'Ingénieur d'État, École Nationale Polytechnique.

[5] Kebede, T., Wondie, Y., Steinbrunn, J., Kassa, H.B. and Kornegay, K.T. (2022) Multi-Carrier Waveforms and Multiple Access Strategies in Wireless Networks: Performance, Applications, and Challenges. *IEEE Access*, **10**, 21120-21140. https://doi.org/10.1109/access.2022.3151360

[6] Oubda, A. (2024) Contribution du numérique dans la stratégie d'insertion de l'économie burkinabè dans les chaînes de valeur nationales et internationales. *Revue internationale des francophonies*,. https://doi.org/10.35562/rif.1577

[7] Alamouti, S.M. (1998) A Simple Transmit Diversity Technique for Wireless Communications. *IEEE Journal on Selected Areas in Communications*, **16**, 1451-1458. https://doi.org/10.1109/49.730453

[8] Rappaport, T.S. (2002) Wireless Communications: Principles and Practice. 2nd Edition, Prentice Hall.

[9] Liu, X., Zhang, X., Zhang, L., Xiao, P., Wei, J., Zhang, H., *et al*. (2020) PAPR Reduction Using Iterative Clipping/Filtering and ADMM Approaches for OFDM-Based Mixed-Numerology Systems. *IEEE Transactions on Wireless Communications*, **19**, 2586-2600. https://doi.org/10.1109/twc.2020.2966600

[10] Håkegård, J.E., Lundkvist, H., Rauniyar, A. and Morris, P. (2024) Performance Evaluation of an Open Source Implementation of a 5G Standalone Platform. *IEEE Access*, **12**, 25809-25819. https://doi.org/10.1109/access.2024.3367120

[11] MathWorks (1996) Communications Toolbox User's Guide. The MathWorks, Inc.

[12] Huawei Technologies Co., Ltd. (2018) BBU BTS5900 Hardware Description. https://www.huawei.com/cn/news/2018/1/Huawei-Turkcell-BBU5900-5G

[13] Lin, S., Costello, D.J., *et al*. (2001) Error Control Coding. Prentice Hall.

[14] Lu, H., Zeng, Y., You, C., Han, Y., Zhang, J., Wang, Z., *et al*. (2024) A Tutorial on Near-Field XL-MIMO Communications toward 6 g. *IEEE Communications Surveys & Tutorials*, **26**, 2213-2257. https://doi.org/10.1109/comst.2024.3387749

[15] Dabone, Y., Zongo, P. and Ouedraogo, T.F. (2025) Network Optimization for Data Flow Control in a Security-Challenged Country: The Case of Burkina Faso. In: Silhavy, R. and Silhavy, P., Eds., *Software Engineering*: *Emerging Trends and Practices in System Development*, Springer, 270-279. https://doi.org/10.1007/978-3-032-00715-5_16

[16] Chen, W., Lin, X., Lee, J., Toskala, A., Sun, S., Chiasserini, C.F., *et al*. (2023) 5G-Advanced toward 6G: Past, Present, and Future. *IEEE Journal on Selected Areas in Communications*, **41**, 1592-1619. https://doi.org/10.1109/jsac.2023.3274037

[17] Wang, C., You, X., Gao, X., Zhu, X., Li, Z., Zhang, C., *et al*. (2023) On the Road to 6G: Visions, Requirements, Key Technologies, and Testbeds. *IEEE Communications Surveys & Tutorials*, **25**, 905-974. https://doi.org/10.1109/comst.2023.3249835